RESEARCH ARTICLE

DOI: 10.34256/famr2522

Frontiers in Advanced Materials Research

Damask Rose-Mediated ZnO/HAp Nanocomposite: A Novel Approach for Biomedical Application

P. Yasotha [a], V. Kalaiselvi [b,*], S. Gopi [c], V. Anusha Devi [a], T. Sarathamani [a]

[a] Department of Physics, Navarasam Arts and Science College for Women, Arachalur, Erode, Tamil Nadu, India

[b] Department of Internet of Things, Vellalar College for women, Thindal, Erode, Tamil Nadu, India.

[c] Department of Physics, Sri Ramakrishna Mission Vidyalaya College of Arts and Science, Coimbatore, India

* Corresponding Author: nk.arthi.kalai@gmail.com

Received: 08-09-2025, Revised: 14-11-2025, Accepted: 25-11-2025, Published: 07-12-2025

Abstract: In this study, zinc oxide/hydroxyapatite (ZnO/HAp) nanocomposites were successfully synthesized via a green method using *Damask rose* extract as a natural reducing and stabilizing agent. The use of this plant extract not only provides an eco-friendly and cost-effective synthesis route but also imparts additional biological functionalities to the nanocomposites due to the presence of bioactive phytochemicals. The synthesized ZnO/HAp nanocomposites were characterized by various analytical techniques. X-ray diffraction (XRD) analysis confirmed the crystalline nature and phase purity of both ZnO and HAp, with well-defined diffraction peaks. Fourier-transform infrared spectroscopy (FTIR) revealed functional groups associated with metal–oxygen bonding as well as organic moieties derived from the plant extract. UV–Visible spectroscopy exhibited strong absorption in the UV region, validating the successful formation of ZnO nanoparticles and highlighting their potential for biomedical optical applications. The antimicrobial performance of the ZnO/HAp nanocomposites was evaluated against different pathogenic strains. Antibacterial activity was significant against both Gram-positive (*Streptococcus mutans*) and Gram-negative (*Fusobacterium nucleatum*) bacteria, as indicated by prominent inhibition zones. Furthermore, antifungal assays demonstrated notable inhibitory effects against *Cryptococcus neoformans*, confirming the broad-spectrum antimicrobial efficacy of the synthesized nanocomposites. The novelty of this work lies in the utilization of *Damask rose* extract for the green synthesis of ZnO/HAp nanocomposites, which not only reduces the reliance on hazardous chemical methods but also enhances the bioactivity of the material, making it a promising candidate for biomedical applications.

Keywords: Antibacterial activity, ZnO/HAp nanocomposites, Green synthesis, XRD, FTIR, UV-Visible.

1. Introduction

The simplest definition of nanotechnology is "technology on the nanoscale." Subsequently, various definitions of nanotechnology have evolved. However, this original definition requires further clarification, particularly regarding the meaning of the nanoscale. Therefore, nanotechnology can be properly defined only by specifying the "nanoscale," which generally refers to dimensions in the range of 1–100 nm [1].Zinc oxide (ZnO) is a semiconductor material with a wide band gap energy of 3.37 eV at room temperature. It has been extensively utilized due to its excellent catalytic, electrical, optoelectronic, and photochemical properties. Owing to their high surface area and enhanced catalytic activity, ZnO nanostructures offer significant advantages in catalytic reaction processes. Since zinc oxide exhibits diverse physical and chemical properties depending on the morphology of its nanostructures, it is essential to investigate not only various synthesis methods but also the resulting physicochemical properties in relation to morphology. ZnO is recognized as a technologically important material with a wide range of applications, including semiconductors, gas sensors, piezoelectric sensors, electroluminescent materials, magnetic materials and actuators, as well as ingredients in cosmetic products [2]. Hydroxyapatite (HAp) is widely employed in biomedical applications, particularly in orthopaedics, odontology, and as a coating material for metallic implants. Natural bone consists of approximately 70% hydroxyapatite, 20% collagen, and 10% water. HAp has the chemical formula $Ca_{10}(PO_4)_6(OH)_2$ rather than $Ca_5(PO_4)_3(OH)$, as the crystal structure contains two formula units per unit cell. According to Boskey, hydroxide deficiency in bone apatite leads to its classification as "hydroxyapatite" or simply "apatite." In addition to its chemical similarity to natural bone, HAp exhibits excellent biocompatibility, strong affinity toward biopolymers, and high osteogenic potential. Consequently, it has been widely used in biomedical applications such as bioactive coatings for metallic osseous implants, middle-ear implants, dental materials, and tissue engineering systems. Numerous studies have demonstrated that HAp can be synthesized in various structures and sizes, and in recent years, nanosized HAp has attracted significant attention among researchers [3].The three fundamental requirements for nanoparticle synthesis include the selection of a green or environmentally friendly solvent, an efficient reducing agent, and a non-toxic stabilizing material. Several synthesis routes have been developed, including physical, chemical, and biological methods. Conventional chemical methods are often expensive and involve the use of hazardous and toxic chemicals, posing serious environmental and health risks. In contrast, the biosynthetic route represents a safe, biocompatible, and environmentally friendly green approach for nanoparticle synthesis, utilizing plants and microorganisms for biomedical applications. This method can be carried out using fungi, algae, bacteria, and plant sources. Various plant parts, such as leaves, fruits, roots, stems, and seeds, have been employed for nanoparticle synthesis due to the presence of phytochemicals that act as reducing and stabilizing agents. In general, nanoparticle synthesis follows two main pathways: top-down and bottom-up approaches [4]. Damask rose (*Rosa damascena* Mill.) (Figure. 1) is a deciduous shrub and one of the most important aromatic, medicinal, and ornamental plants. It is the most valuable

Rosa species cultivated for the production of rose water and rose oil, which are extensively used in the perfume industry and as flavoring agents in food products. Damask rose is a hybrid derived from two groups: autumn damasks and summer damasks. Autumn damasks, which include Portland roses, are shorter and more compact and possess the ability to rebloom in autumn, producing flowers in red shades. In contrast, summer damasks bloom only once, have more open thorn arrangements, and grow as shrubs bearing flowers with intense pink to white coloration. Damask rose belongs to the family Rosaceae. The genus *Rosa* comprises more than 200 species and approximately 18,000 cultivars worldwide. Known as the "king of flowers," the damask rose has symbolized love, purity, faith, and beauty since ancient times. Although there is considerable disagreement regarding the exact number of rose species, roses generally occur as erect shrubs, climbers, or trailing plants with stems typically armed with sharp prickles. Rose flowers vary widely in form and size and are generally large and attractive, displaying colors ranging from white and yellow to red. Most rose species are native to Asia, with a few originating from North America, Europe, and Northwestern Africa. Roses have significant cultural importance across various societies and occur in diverse growth forms, from compact miniature roses to climbing varieties. Damask rose plants can grow up to approximately 7 m in height. Extensive development of garden roses has occurred due to the ease of hybridization among different species [5].

Figure 1. Damask Rose Flower

2. Experiment Producer

2.1 Materials Needed

Zinc acetate dehydrate ($Zn(CH_3COO)_2.2H_2O$), Calcium Hydroxide($Ca(OH)_2$) and Orthophosphoric acid(H_3PO_4) chemicals were purchased in company of scientific & chemicals, Erode, Sigma brand and Analytical grade solution. The fresh Damask rose petals were collected from Erode. These petals used as a green reducing and stabilizing agent.

2.2 Preparation of Rose Petals Extract

Dark Pink Damask Rose flowers were collected in encompassing areas. The flowers were washed periodically with distilled water to remove the dust particles. Then, the rose petals extricated by taking 30gm petals with 150ml distilled water. It was boiled for 30minutes and kept at 70°C, the colour of emulsion is changed to vivid purplish red colour.

2.3 Synthesis of Pure ZnO and HAp Nanocomposite

The pure HAp nanoparticle were prepared by 3gm of Calcium Hydroxide with 75ml distilled water and it was stirred for ½ minutes by magnetic stirrer.1.5ml of Ortho Phosphoric acid with 75ml distilled water and it was stirred for ½ minutes by magnetic stirrer. The prepared two solutions stirred for ½ minutes maintained with pH of 12 by adding drop by drop of 1gm NaOH. After maintaining of PH it stirred for ½ minutes, the white colour aqueous solution of HAp is formed. Pure ZnO nanoparticles were prepared by 3gm of Zinc Acetate dihydrate with 75ml of distilled water and it was stirred for ½ minutes by magnetic stirrer. Maintaining the PH of 12 by adding 2gm NaOH and stirrer for ½ minutes. The colorless ZnO solution is formed.

2.4 Preparation of ZnO: HAp nanocomposites with Flower Extracts

The above prepared solutions of ZnO and HAp is mixed and the solution is dissolved in 20ml of Damask Rose extract. The solution was stirred for ½ minutes, it will turn into light yellow colour (sandal). Then, the solution was undisturbed for 24Hrs.The settled solution was kept in hot air oven at 70°C for 3Hrs.Finally,the lightly yellow colour (sandal) powder is comes out.

2.5 Chemical Reaction

2.5.1 Pure Zinc Oxide (Zno) Formation

$$Zn(CH_3COO)_2 + 2NaOH \longrightarrow Zn(OH)_2 + 2CH_3COONa$$

$$Zn(OH)_2 \longrightarrow ZnO + H_2O$$

2.5.2 Pure Hydroxyapatite (HAp) Formation

$$10Ca(OH)_2 + 6H_3PO_4 \longrightarrow Ca_{10}(PO_4)_6(OH)_2 + 18H_2O$$

2.5.3 Formation of ZnO/HAp Nanocomposite

$$ZnO + Ca_{10}(PO_4)_6(OH)_2 \xrightarrow{\text{with + Rosadamascena ectract}} \text{ZnO/HAp Nanocomposite}$$

2.6 Characterization Techniques

The optical properties of the synthesized ZnO/HAp nanocomposites were analyzed using a UV-Visible spectrometer (model: Shimadzu UV-1800) in the wavelength range of 200-800 nm.XRD analysis was performed using an X-ray diffraction (model scintag XDS-2000) with Cu-Kα radiation (λ=1.5406Å) to determine the crystallographic structure of the nanocomposites. FTIR spectra were recorded using a Shimadzu Prestige-21 FTIR spectrometer in the range 4000 to 400 cm^{-1} to identify functional group.

2.7 Anti-bacterial Activity

Gram-positive and Gram-negative bacteria are commonly used as model microorganisms to evaluate the antimicrobial efficacy of novel materials due to their distinct cell wall structures and pathogenic behavior. *Streptococcus mutans* is a Gram-positive, facultative anaerobic bacterium that is predominantly associated with dental caries and oral biofilm formation [6]. It adheres strongly to tooth surfaces and produces extracellular polysaccharides from dietary sugars, leading to biofilm development and acid production. The acidic microenvironment created by *S. mutans* causes demineralization of tooth enamel, making it one of the primary etiological agents of dental caries. Owing to its thick peptidoglycan layer and absence of an outer membrane, *S. mutans* exhibits characteristic susceptibility patterns that are useful for assessing antibacterial mechanisms against Gram-positive bacteria [9].*Fusobacterium nucleatum* is a Gram-negative, obligate anaerobic bacterium commonly found in the human oral cavity and is strongly associated with periodontal diseases. It plays a key role as a "bridge organism" in dental plaque by facilitating co-aggregation between early and late colonizing bacterial species. The presence of an outer membrane rich in lipopolysaccharides (LPS) contributes to its virulence, inflammatory potential, and enhanced resistance to antimicrobial agents [7]. *F. nucleatum* has also been implicated in systemic infections and has been linked to colorectal cancer and adverse pregnancy outcomes. Due to its thin peptidoglycan layer and complex outer membrane structure, it serves as a representative model for evaluating antibacterial activity against Gram-negative bacteria.The selection of *S. mutans* and *F. nucleatum* provides a comprehensive understanding of antimicrobial performance against both Gram-positive and Gram-negative bacterial strains, thereby offering valuable insights into the potential biomedical and dental applications of newly developed materials [8].

3. Results and Discussion

3.1 Structural Properties

X-ray diffraction (XRD) non-destructive techniques used to analyze the crystalline structure of materials by measuring the angles and intensities of X-ray diffracted from a sample, providing information about its atomic arrangement phase composition and other structural properties. The XRD patterns of the ZnO/HAp composites prepared by Sol-Gel methods are shown in figure-3.1. From the XRD patterns and the corresponding characteristic 2θ values of the diffractions peaks, it can be confirmed that ZnO/HAp samples is identified as hexagonal phases(JCPDS-09-0532,36-1451) [10]. The X-ray diffraction (XRD) pattern of the ZnO/HAp nanocomposite confirms the successful formation of a biphasic system consisting of crystalline zinc oxide (ZnO) and hydroxyapatite (HAp) [11]. The prominent diffraction peaks observed at 2θ values around 31.7°, 34.4°, 36.2°, 47.5°, 56.6°, and 62.8° correspond to the (100), (002), (101), (102), (110), and (103) planes of hexagonal wurtzite ZnO, which are in good agreement with the standard JCPDS card No. 36-1451, indicating the high crystallinity of ZnO nanoparticles [12]. Additionally, characteristic diffraction peaks appearing at approximately 25.9°, 31.8°, 32.9°, 34.1°, 39.8°, 46.7°, and 49.5° are indexed to the (002), (211), (300), (202), (310), (222), and (213) planes of hexagonal hydroxyapatite, matching well with JCPDS card No. 09-0432. The coexistence of both ZnO and HAp diffraction peaks without any secondary impurity phases confirms the successful incorporation of ZnO into the HAp matrix.The slight peak broadening observed in the diffraction pattern suggests the nanocrystalline nature of the composite, while minor peak shifts indicate possible lattice strain and interfacial interaction between ZnO and HAp. The average crystallite size, calculated using the Debye–Scherrer equation, falls within the nanoscale range, further supporting the formation of ZnO/HAp nanocomposites suitable for biomedical applications such as bone tissue engineering and anticancer therapy [13].

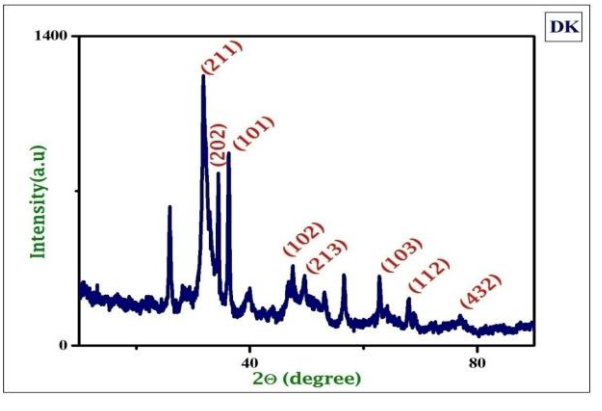

Figure 2. XRD pattern of ZnO/HAp composite synthesized using Damask Rose Flower extract

3.2 Functional group Analysis

The Fourier transform infrared (FTIR) spectrum of the ZnO/HAp nanocomposite confirms the successful formation of hydroxyapatite and its interaction with ZnO nanoparticles. The broad absorption band observed at around 3330–3340 cm^{-1} is attributed to the stretching vibration of –OH groups, arising from structural hydroxyl groups of hydroxyapatite and adsorbed moisture. The weak band near 2970–2980 cm^{-1} corresponds to C–H stretching vibrations, which may originate from residual organic moieties derived from the green synthesis route or surface-bound phytochemicals [14].The absorption band appearing at approximately 1410–1420 cm^{-1} is assigned to the ν_3 asymmetric stretching mode of CO_3^{2-} ions, indicating partial carbonate substitution within the HAp lattice, a characteristic feature of biologically relevant hydroxyapatite. The peak around 1210–1220 cm^{-1} is associated with **P**–O stretching vibrations of the phosphate (PO_4^{3-}) group [15]. Furthermore, the strong absorption band observed near 840–875 cm^{-1} corresponds to the $\boldsymbol{\nu_2}$ bending mode of PO_4^{3-} ions, confirming the presence of crystalline hydroxyapatite.The characteristic Zn–O stretching vibration, typically appearing below 500 cm^{-1}, overlaps with the phosphate bending region and indicates the incorporation of ZnO into the HAp matrix. The coexistence of phosphate, hydroxyl, carbonate, and Zn–O related bands without additional impurity peaks confirms the successful synthesis of the ZnO/HAp nanocomposite and suggests strong interfacial interactions between ZnO nanoparticles and the hydroxyapatite framework, which are beneficial for biomedical and anticancer applications [16].

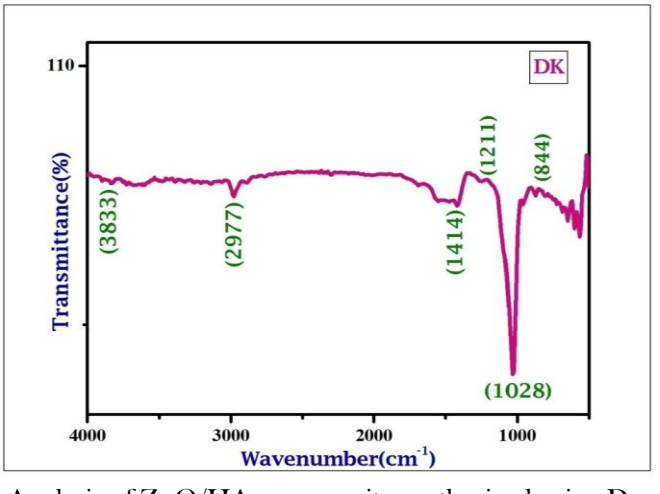

Figure 3. FTIR Analysis of ZnO/HAp composite synthesized using Damask Rose Flower extract

3.3 Optical Properties

The UV–Visible absorption spectrum of the synthesized ZnO/HAp nanocomposite was recorded in the wavelength range of 200–800 nm, as shown in Figure 4,5. The spectrum exhibits

a strong absorption band centered at approximately 309 nm**,** which is attributed to the intrinsic band-to-band electronic transition of ZnO nanoparticles [17]**.** This absorption peak corresponds to the excitation of electrons from the valence band to the conduction band, confirming the formation of nanoscale ZnO within the hydroxyapatite matrix.

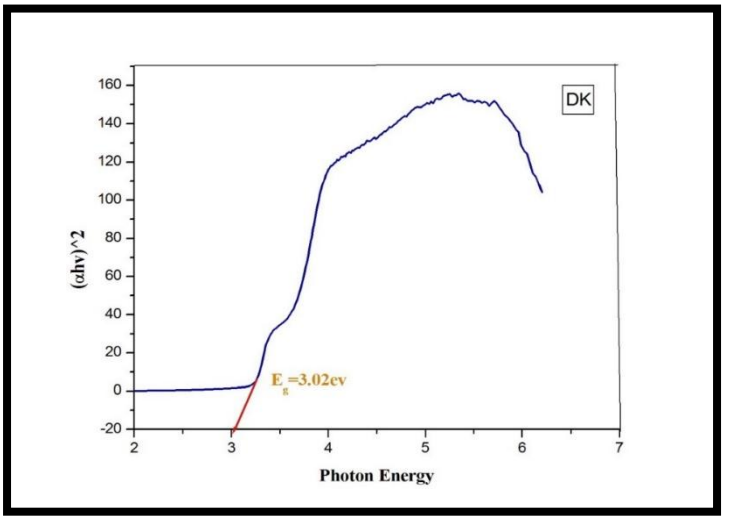

Figure 4. UV-Vis Spectrum of Tauc plot ZnO/HAp composite Synthesized of Damask Rose flower extract

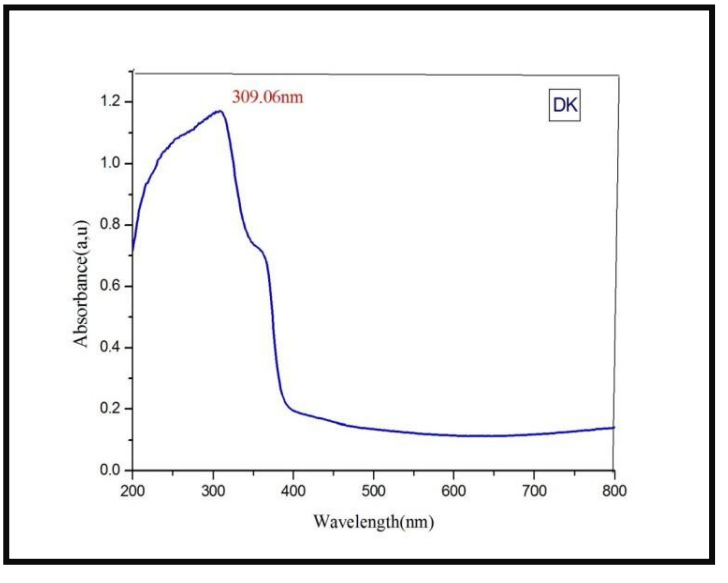

Figure-5. UV-Visible Spectrum of ZnO/HAp composite Synthesized using Damask Rose flower extract

The sharp absorption edge observed in the near-UV region indicates the high crystallinity and nanosized nature of ZnO particles. The slight red shift of the absorption maximum compared to bulk ZnO (≈ 370 nm) suggests strong interfacial interaction between ZnO and hydroxyapatite, as well as possible quantum confinement effects arising from reduced particle size [18]. Furthermore, the low absorbance in the visible region (400–800 nm) reflects the optical transparency of the composite, which is advantageous for biomedical and photocatalytic applications.

The optical band gap energy of the ZnO/HAp nanocomposite was estimated using the Tauc plot method by extrapolating the linear region of the $(\alpha h\nu)^2$ versus $h\nu$ plot. The calculated band gap value confirms the semiconducting behavior of the composite and demonstrates that the incorporation of HAp does not disturb the fundamental electronic structure of ZnO, while improving its biocompatibility and functional performance [19].

3.4 Antibacterial Activity

The antibacterial activity of the synthesized ZnO/HAp nanocomposite was evaluated using the agar well diffusion method against Gram-positive *Streptococcus mutans* and Gram-negative *Fusobacterium nucleatum*, as illustrated in Figures 6 and 7. The nanocomposite exhibited a clear concentration-dependent inhibitory effect against both bacterial strains. At higher concentrations, a significantly larger zone of inhibition (ZOI) was observed, indicating enhanced antibacterial efficacy of the ZnO/HAp nanocomposites [20]. Notably, the nanocomposite showed stronger antibacterial activity against *Streptococcus mutans* compared to *Fusobacterium nucleatum*, which can be attributed to differences in cell wall structure between Gram-positive and Gram-negative bacteria.

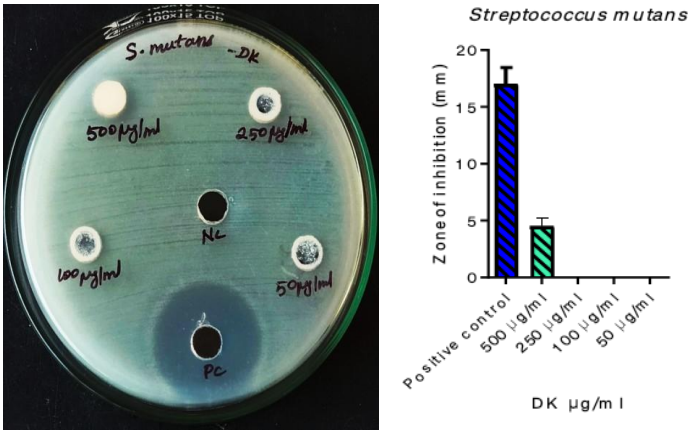

Figure 6. Effect of sample against Streptococcus mutans

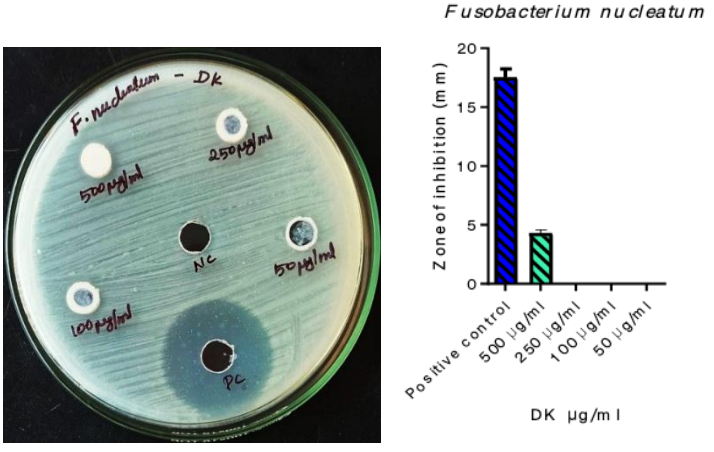

Figure 7. Effect of sample against Fusobacterium nucleatum

The enhanced antibacterial performance is mainly associated with the synergistic action of ZnO nanoparticles and hydroxyapatite**,** where ZnO contributes to the generation of reactive oxygen species (ROS) and Zn^{2+} ion release**,** leading to membrane disruption, protein denaturation, and bacterial cell death. Meanwhile, hydroxyapatite provides a large surface area and promotes better dispersion of ZnO, facilitating increased interaction with bacterial cells. The presence of a measurable inhibition zone even at lower concentrations demonstrates the broad-spectrum antibacterial potential of the ZnO/HAp nanocomposites [21]. These results confirm that the synthesized nanocomposite is a promising antibacterial agent, particularly for oral pathogens, supporting its potential application in biomedical coatings, dental materials, bone tissue engineering, and infection-associated bone cancer therapy**.**

3.5 Anti-Fungal Activity

The antifungal efficacy of the synthesized ZnO/HAp nanocomposite (DK) was evaluated against *Cryptococcus neoformans* using the agar well diffusion method, as illustrated in Figure X. The nanocomposite exhibited a clear and concentration-dependent antifungal activity, as evidenced by the increasing zone of inhibition (ZOI) with increasing sample concentration (50–500 µg/mL). The highest concentration (500 µg/mL) produced a prominent inhibition zone, comparable to the positive control, while lower concentrations (250, 100, and 50 µg/mL) showed moderate but distinct inhibitory effects. The observed antifungal activity can be attributed to the synergistic interaction between ZnO nanoparticles and hydroxyapatite [22]. ZnO is known to induce antifungal action through the generation of reactive oxygen species (ROS) and the release of Zn^{2+} ions, which disrupt fungal cell membranes, alter intracellular enzyme activity, and damage nucleic acids. Hydroxyapatite enhances the dispersion and stability of ZnO nanoparticles, facilitating increased surface contact with fungal cells and improving overall antifungal performance.

The effective inhibition of *C. neoformans*, a clinically significant opportunistic fungal pathogen, highlights the broad-spectrum antimicrobial potential of the ZnO/HAp nanocomposites [23]. These results suggest that the synthesized nanocomposite is a promising candidate for biomedical applications, particularly in bone-related infections, implant coatings, and infection-associated cancer therapy, where antifungal protection is essential.

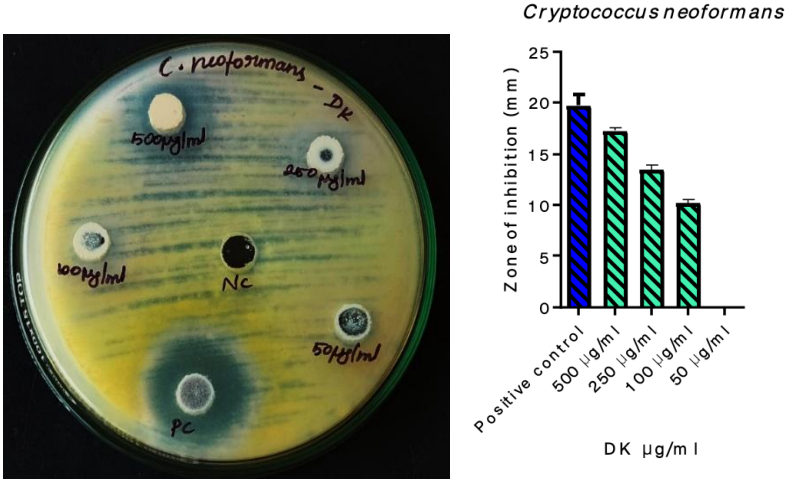

Figure 8. Effect the sample of Cryptococcus neoforma

4. Conclusion

In this work, the synthesized hydroxyapatite–zinc oxide (HAp:ZnO) nanocomposite was systematically characterized using X-ray diffraction (XRD), Fourier transform infrared spectroscopy (FTIR), and ultraviolet–visible (UV–Vis) spectroscopy to investigate its structural, functional, and optical properties. In addition, the antibacterial and antifungal activities of the nanocomposite were evaluated to assess its potential biomedical applications. X-ray diffraction (XRD) analysis was employed to determine the crystalline nature and phase composition of the HAp:ZnO nanocomposite. The diffraction peaks confirmed the successful formation of crystalline HAp and ZnO phases without any secondary impurities. The average crystallite size of the nanocomposite was calculated using the Debye–Scherrer equation, indicating nanoscale dimensions that are favorable for biological applications. Fourier transform infrared (FTIR) spectroscopy was used to identify the functional groups present in the synthesized nanocomposite. The FTIR spectrum exhibited characteristic absorption bands corresponding to phosphate (PO_4^{3-}) groups of hydroxyapatite and Zn–O stretching vibrations of zinc oxide. The presence of these functional groups confirms the successful incorporation of ZnO into the HAp matrix and suggests strong interfacial interactions between the components. Ultraviolet–visible (UV–Vis) spectroscopy was carried out to study the optical properties of the HAp:ZnO

nanocomposite. The absorption spectrum revealed a characteristic absorption edge in the UV region, attributed to ZnO. The optical band gap energy was estimated using Tauc's plot, demonstrating that the nanocomposite possesses suitable electronic properties for photocatalytic and biomedical applications. Furthermore, the antibacterial and antifungal activities of the HAp:ZnO nanocomposite were investigated against selected pathogenic microorganisms. The results demonstrated enhanced antimicrobial efficacy, which can be attributed to the synergistic effect of ZnO nanoparticles and hydroxyapatite. The generation of reactive oxygen species (ROS) and the interaction of Zn^{2+} ions with microbial cell membranes are considered responsible for the observed antimicrobial activity. Overall, the structural, optical, and biological studies confirm that the synthesized HAp:ZnO nanocomposite exhibits promising properties for potential applications in biomedical fields, particularly in antimicrobial coatings and bone tissue engineering.

References

[1] M. Nasrollahzadeh, S.M. Sajadi, M. Sajjadi, Z. Issaabadi, An introduction to nanotechnology. In Interface science and technology, 28, (2019) 1-27. https://doi.org/10.1016/B978-0-12-813586-0.00001-8

[2] P. Uikey, K. Vishwakarma, Review of zinc oxide (ZnO) nanoparticles applications and properties. International Journal of Emerging Technology in Computer Science & Electronics, 21(2), (2016) 239-242.

[3] P.N. M.u'ad, R.A. Haq, H.M. Noh, H.Z. Abdullah, M.I. Idris, T.C. Lee, Synthesis method of hydroxyapatite: A review. Materials Today: Proceedings, 29, (2020) 233-239. https://doi.org/10.1016/j.matpr.2020.05.536

[4] S. Jadoun, R. Arif, N.K. Jangid, R.K. Meena, Green synthesis of nanoparticles using plant extracts: A review. Environmental Chemistry Letters, 19(1), (2021) 355-374. https://doi.org/10.1007/s10311-020-01074-x

[5] F. Shabbir, M.A. Hanif, M.A. Ayub, M.I. Jilani, S. Rahman, Damask rose. In Medicinal plants of South Asia, (2020) 217-230. https://doi.org/10.1016/B978-0-08-102659-5.00017-3

[6] W. J. Loesche, Role of Streptococcus mutans in human dental decay. Microbiological reviews, 50(4), (1986) 353-380. https://doi.org/10.1128/mr.50.4.353-380.1986

[7] P.E. Kolenbrander, R.J. Palmer, S. Periasamy, N.S. Jakubovics, Oral multispecies biofilm development and the key role of cell–cell distance. Nature Reviews Microbiology, 8(7), (2010) 471-480. https://doi.org/10.1038/nrmicro2381

[8] Y.W. Han, (2015). Fusobacterium nucleatum: a commensal-turned pathogen. Current opinion in microbiology, 23, 141-147. https://doi.org/10.1016/j.mib.2014.11.013

[9] W.H. Bowen, H.J.C.R. Koo, Biology of Streptococcus mutans-derived glucosyltransferases: role in extracellular matrix formation of cariogenic biofilms. Caries research, 45(1), (2011) 69-86. https://doi.org/10.1159/000324598

[10] V. Stengl, S. Bakardjieva, N. Murafa, V. Houšková, K. Lang, Visible-light photocatalytic activity of TiO2/ZnS nanocomposites prepared by homogeneous hydrolysis. Microporous and Mesoporous Materials, 110(2-3), (2008) 370-378. https://doi.org/10.1016/j.micromeso.2007.06.052

[11] S.V. Dorozhkin, Calcium orthophosphates: occurrence, properties, biomineralization, pathological calcification and biomimetic applications. Biomatter, 1(2), (2011) 121-164. https://doi.org/10.4161/biom.18790

[12] Ramesh, S., Z.Z. Loo, C.Y. Tan, W.J. Kelvin Chew, Y.C. Ching, F. Tarlochan, H. Chandran, S. Krishnasamy, L.T. Bang, Ahmed A.D. Sarhan, Characterization of biogenic hydroxyapatite derived from animal bones for biomedical applications. Ceramics International, 44(9), (2018) 10525-10530. https://doi.org/10.1016/j.ceramint.2018.03.072

[13] B.D. Cullity, R. J. P. T. Smoluchowski, Elements of X-ray Diffraction. Physics Today, 10(3), (1957) 50-50.

[14] S.K. Krishnan, E. Singh, P. Singh, M. Meyyappan, H.S.Nalwa, A review on graphene-based nanocomposites for electrochemical and fluorescent biosensors. RSC advances, 9(16), (2019) 8778-8881. https://doi.org/10.1039/C8RA09577A

[15] S. Koutsopoulos, Synthesis and characterization of hydroxyapatite crystals: a review study on the analytical methods. Journal of Biomedical Materials Research, 62(4), (2002) 600-612. https://doi.org/10.1002/jbm.10280

[16] S.V. Dorozhkin, Bioceramics of calcium orthophosphates. Biomaterials, 31(7), (2010) 1465-1485. https://doi.org/10.1016/j.biomaterials.2009.11.050

[17] U. Ozgür, Y.I. Alivov, C. Liu, A. Teke, M.A. Reshchikov, S. Doğan, V. Avrutin, S. J. Cho, A.H. Morkoç, A comprehensive review of ZnO materials and devices. Journal of applied physics, 98(4), (2005) 041301. https://doi.org/10.1063/1.1992666

[18] O.O. Martynyuk, L.F. Sukhodub, A.M. Meshkov, L.B. Sukhodub, Structural properties of the ZnO doped hydroxyapatite nanocomposite material, 2016 International Conference on Nanomaterials: Application & Properties (NAP), Lviv, Ukraine, 2016, pp. 02NSA07-1-02NSA07-5. https://doi.org/10.1109/NAP.2016.7757308

[19] R. Maind, S. Halder, A.R. Bhat, D. Bhattacharya, M.H. Mujahid, A. Abu-Rayyan, M. Iqbal, V.J. Upadhye, S. Ahmed, M.r Alam, G. Tataringa, Biomimetic green synthesis of ZnO nanoparticles using Cheilocostus speciosus and Gardenia gummifera with comprehensive characterization and bioactivity assessment. Scientific Report, 15 (2025) 44323. https://doi.org/10.1038/s41598-025-30720-z

[20] A. Sirelkhatim, S. Mahmud, A. Seeni, N.H.M. Kaus, L.C. Ann, S.K.M. Bakhori, H. Hasan, D. Mohamad, Review on zinc oxide nanoparticles: antibacterial activity and toxicity mechanism. Nano-micro letters, 7(3), (2015) 219-242. https://doi.org/10.1007/s40820-015-0040-x

[21] K.R. Raghupathi, R.T. Koodali, A.C. Manna, Size-dependent bacterial growth inhibition and mechanism of antibacterial activity of zinc oxide nanoparticles. Langmuir, 27(7), (2011) 4020-4028. https://doi.org/10.1021/la104825u

[22] K.R. Raghupathi, R.T. Koodali, A.C. Manna Size-dependent antimicrobial activity of zinc oxide nanoparticles. Langmuir, 27(7), (2011) 4020–4028. https://doi.org/10.1021/la104825u

[23] D.K. Stein, A.M. Sugar, Fungal infections in the immunocompromised host. Diagnostic Microbiology and Infectious Disease, 12(4 Suppl), (1989) 221S-228S.

Conflict of interest: The Authors have no conflicts of interest to declare that they are relevant to the content of this article.